Reply to Anonymous Referee #2

→ Specific changes have been made in response to the reviewer's comments and are described below. The reviewer's comments are recalled in blue and changes in the revised version are highlighted in yellow.

Review of „Supercooled liquid water clouds observed over Dome C, Antarctica: temperature sensitivity and surface radiation impact" by Ricaud et al.

The authors investigate the radiative impact of SCLW clouds at Dome C. In general, the topic is very interesting and suitable for ACP and the paper is well written. However, I have some concerns regarding the methodology and recommend major revision.

→ Thank you for your positive remarks in order to increase the quality of the manuscript. All your comments have been taken into account. An in-depth study has been performed to evaluate the choice of the clear-sky reference.

Major comments:

Estimating clear sky surface radiation: Instead of averaging the observations of the complete day, the authors could fit a sinus function to the clear sky observations to account for the diurnal cycle. Likely, this would reduce the bias of up to 20 w/m2 that can be seen in Fig. 4, top panel. Also, when using averaged observations instead of a radiative transfer model to estimate clear sky radiation, the authors should quantify the uncertainties caused by varying temperature and aerosol profiles among the elected clear sky days. A radiative transfer model would be required for this which leaves the question why such a model is not used in the first place.

→ This point has been studied in detail and according to concurring comments from the Reviewer #1. We have performed, using several data sets, an in-depth study to evaluate the surface radiation components in clear-sky conditions. We therefore reproduce below our common response to the two Reviewers.

1) Supplementary data sets

In order to evaluate the surface radiation in clear-sky conditions at Concordia, we have used, in complement to BSRN observations, and at the closest location to Concordia station, two different data sets of surface radiations from:

a) the European Center for Medium-Range Weather Forecasts Reanalysis version 5 (**ERA5**). ERA5 is a climate reanalysis dataset, covering the period 1979 to present. ERA5 is being developed through the Copernicus Climate Change Service (C3S). Extracted data (https://cds.climate.copernicus.eu/cdsapp#!/dataset/reanalysis-era5-single-levels) used here are hourly at a regular horizontal grid of 0.25°x0.25° in clear-sky conditions: surface solar and thermal infrared, downward and net radiations. As explained on the ERA5 website, clear-sky radiations are computed for the same atmospheric conditions of temperature, humidity, ozone, trace gases and aerosol as the corresponding total-sky quantities (clouds included), but assuming that the clouds are not there.

b) the Clouds and the Earth's Radiant Energy System (**CERES**), containing SYN1deg (Hourly CERES and geostationary (GEO) TOA fluxes, MODIS/VIIRS and GEO cloud properties, MODIS/VIIRS aerosols, and Fu-Liou radiative transfer surface and in-atmospheric (profile) fluxes consistent with the CERES observed TOA fluxes, as explained on https://ceres.larc.nasa.gov/data/). Surface fluxes in SYN1deg are computed with cloud properties derived from MODIS and geostationary satellites (GEO), where each geostationary satellite instrument is calibrated against MODIS (Doelling et al. 2013; 2016) at 1°x1° horizontal resolution (https://ceres.larc.nasa.gov/data/). Aerosol and atmospheric data were included as inputs to calculate the radiation flux.

References:

https://ceres.larc.nasa.gov/documents/DQ_summaries/CERES_SYN1deg_Ed4A_DQS.pdf

Doelling, D. R., N. G. Loeb, D. F. Keyes, M. L. Nordeen, D. Morstad, C. Nguyen, B. A. Wielicki, D. F. Young, M. Sun, 2013: Geostationary Enhanced Temporal Interpolation for CERES Flux Products, *Journal of Atmospheric and Oceanic Technology*, **30**(6), 1072-1090. doi: 10.1175/JTECH-D-12-00136.1.

Doelling, D. R., M. Sun, L. T. Nguyen, M. L. Nordeen, C. O. Haney, D. F. Keyes, P. E. Mlynczak, 2016: Advances in Geostationary-Derived Longwave Fluxes for the CERES Synoptic (SYN1deg) Product, *Journal of Atmospheric and Oceanic Technology*, **33**(3), 503-521. doi: 10.1175/JTECH-D-15-0147.1.

2) Comparison between ERA5, CERES and BSRN data.

We have compared the CERES and ERA5 data with the BSRN hourly-averaged data on the 5 reference days (clear-sky conditions) for the Net, LWD, LWU, SWD and SWU SRs. Figure R1 shows these variables for the 26 December 2021. The LWD and LWU values show an overall consistency between ERA5 and CERES (of the order of ~10 W m^{-2}), while a systematic negative bias of ~20-40 W m^{-2} is observed with respect to BSRN data. However, the net longwave radiation, i.e. the difference LWD – LWU for each data set, is reduced to around 5 W m^{-2}. The SWD and SWU signals from ERA5, CERES and BSRN show a similar diurnal variation with differences less than 50 W m^{-2}. When considering the Net SR, some obvious differences up to 50 W m^{-2} can be seen between BSRN, ERA5 and CERES. Since the net longwave radiation is within 10 W m^{-2} for the three data sets, the source of this difference therefore should come from either SWD or SWU radiation.

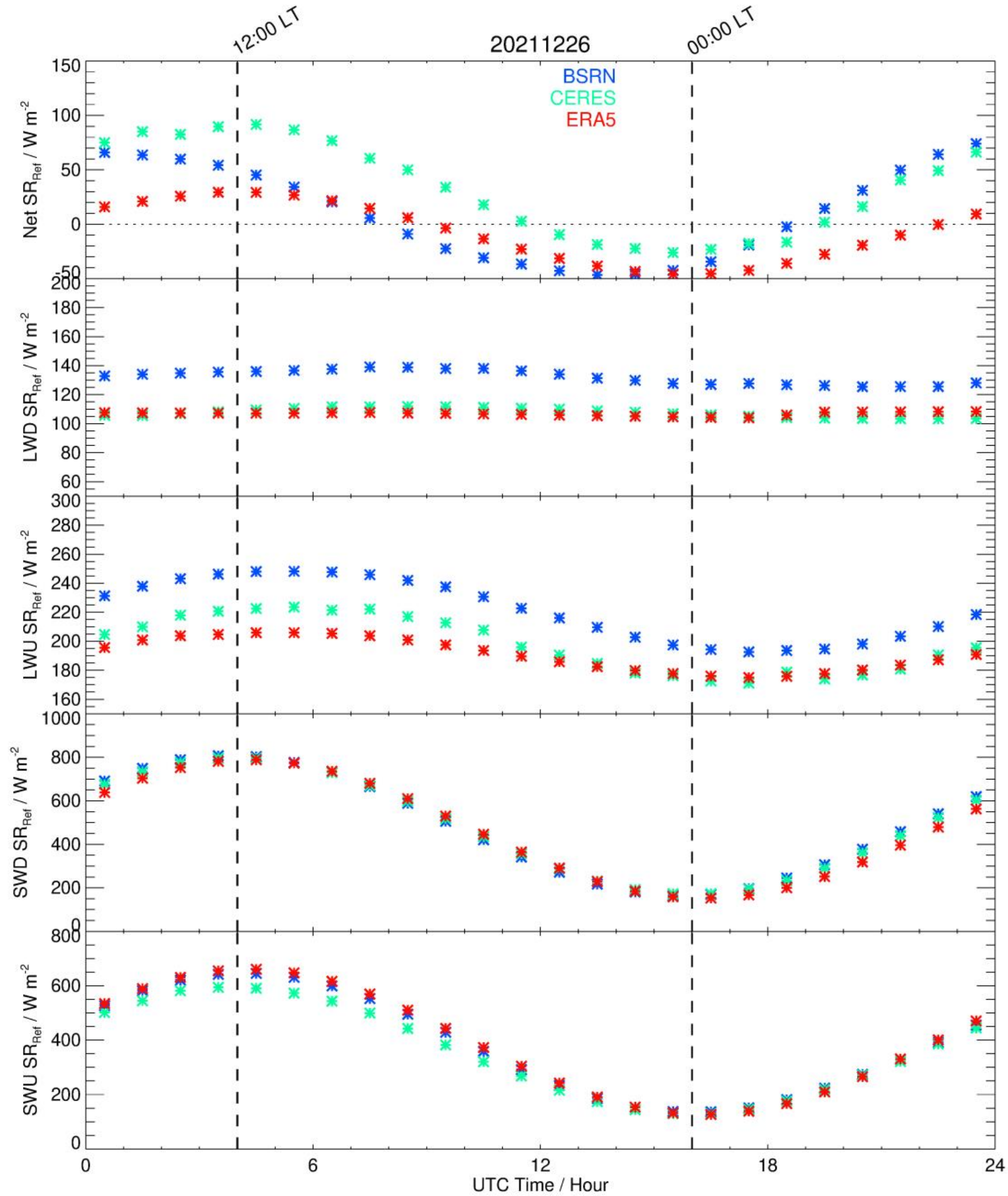

Figure R1. *Hourly time evolution (UTC, hour) of the clear-sky surface radiations (SR, W m^{-2}) observed by the BSRN instruments (blue asterisks), the CERES (green asterisks) and the ERA5 (red asterisks) data sets on 26 December 2021: (from top to bottom) Net SR, Longwave Downward (LWD SR), Longwave Upward (LWU SR), Shortwave Downward (SWD SR) and Shortwave Upward (SWU SR) surface radiations. The 00:00 and 12:00 local times (LT) are highlighted by 2 vertical dashed lines.*

<u>3) Impact of the local albedo on shortwave radiation.</u>

We have calculated, for BSRN, ERA5 and CERES data, the albedo defined as:

Albedo=SWU/SWD.

Figure R2 shows the diurnal evolution of the albedo on 26 December 2021 (clear-sky day). The CERES and ERA5 albedos do not show any significant diurnal variation with quite constant values of 0.74 and 0.83, respectively, whilst the observed BSRN albedo shows a clear diurnal signal with a maximum of 0.85 from 10:00 to 14:00 UTC (from 18:00 to 22:00 LT) and a minimum of 0.70 from 19:00 to 23:00 UTC (from 03:00 to 07:00 LT). The large diurnal signal present in the observed albedo is likely the signature of the sastrugi effect that is obviously absent in the ERA5 and CERES data sets. The BSRN SWU sensor has a circular footprint. For a sensor installed at a height *h* above the ground, 90% of the signal comes from an area at the surface closer than 3.1 *h* (Kassianov et al., 2014). Since at Dome-C the instrument is installed at a height of 2-3 m, the albedo is thus determined by the surface elements in the immediate vicinity (a few meters) of the sensor.

Kassianov E, Barnard J, Flynn C, Riihimaki L, Michalsky J, Hodges G (2014) Areal-averaged spectral surface albedo from ground-based transmission data alone: toward an operational retrieval. Atmosphere 5:597–621. https://doi.org/10.3390/atmos503059)

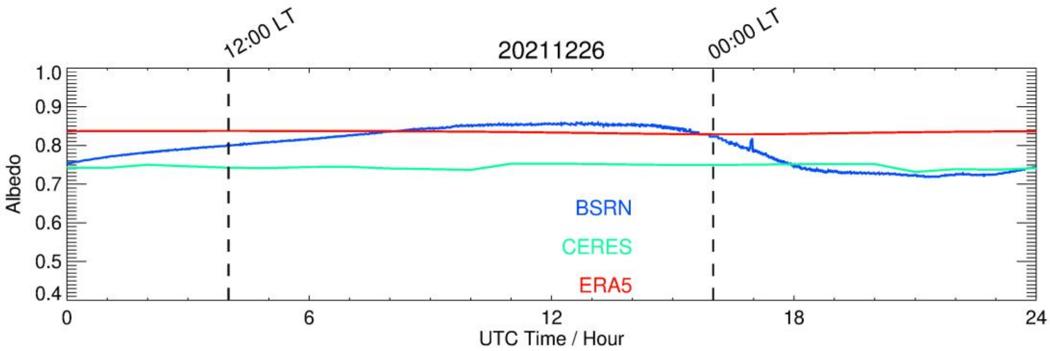

Figure R2. *Time evolution (UTC, hour) of the surface albedo observed by the BSRN sensors (blue), the CERES (green) and the ERA5 (red) data sets on 26 December 2021. The 00:00 and 12:00 local times (LT) are highlighted by 2 vertical dashed lines.*

4) Impact of sastrugi on the albedo.

Sastrugi (Figure R3) are features formed by erosion of snow by wind. They are found in polar regions, and in snowy, wind-swept areas of temperate regions, such as frozen lakes or mountain ridges. Sastrugi are distinguished by upwind-facing points, resembling anvils, which move downwind as the surface erodes.

Figure R3. *Image of sastrugi on the ice surface.*

Figure R4 presents a satellite image showing the Concordia station. The sastrugi are clearly visible producing bright and dark straight lines with a 150°-330° orientation (wrt the N-S axis) (corresponding to solar azimuthal angles at ~13:00 and 01:00 LT). As a consequence, the albedo observed in BSRN is likely dependent of the sastrugi orientation, the sun elevation and the azimuthal angle.

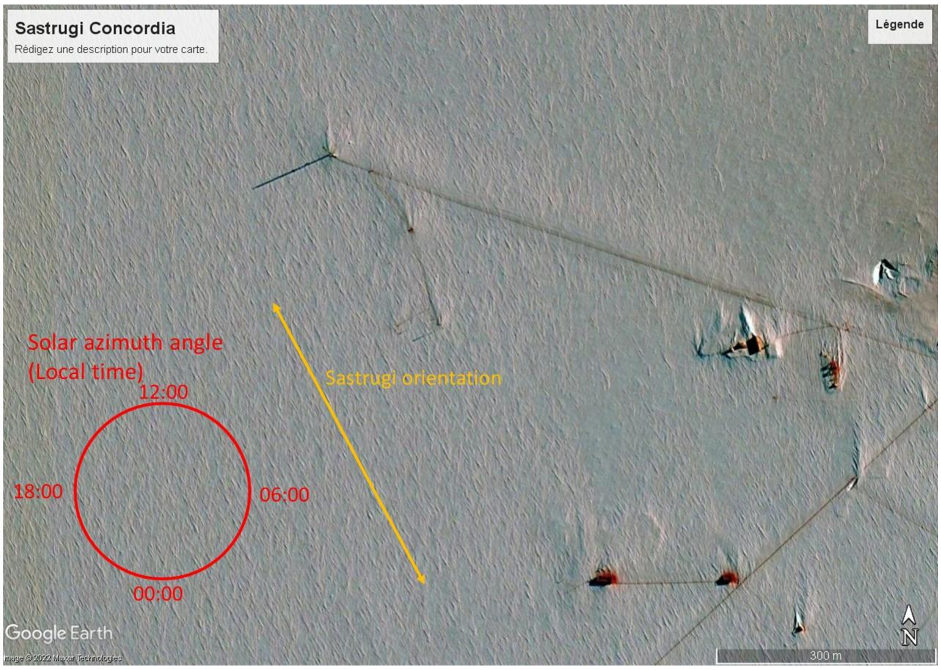

Figure R4. *Images taken from Google Earth showing the Concordia station on the right-hand side. The sastrugi effect producing bright and dark straight lines is clearly visible with one main orientation at ~330° orientation (~11:00 local time solar azimuth angle, with 0° orientation towards the North).*

If we suppose that the sastrugi effect impacts mostly SWU rather than SWD, and the albedo calculated from BSRN observations is the "truth", we can calculate a modified SWU* (including the sastrugi effect) for the ERA5 and CERES as:

SWU(ERA5)*=SWD(ERA5) x albedo(BSRN)
SWU(CERES)*=SWD(CERES) x albedo(BSRN)

Then we calculate the modified Net SR* (including the sastrugi effect) considering SWU* for ERA5 and CERES. As an example, we present Figure R5, similar to Figure R1, in which we added the albedo and the SWU* and Net SRs* (including the sastrugi effect) for CERES and ERA5 (solid lines). We observe that the Net SR* for ERA5 and CERES now coincides with the BSRN Net SR to within 5 W m^{-2}, compared to differences up to 50 W m^{-2} found when the sastrugi effect was not taken into account.

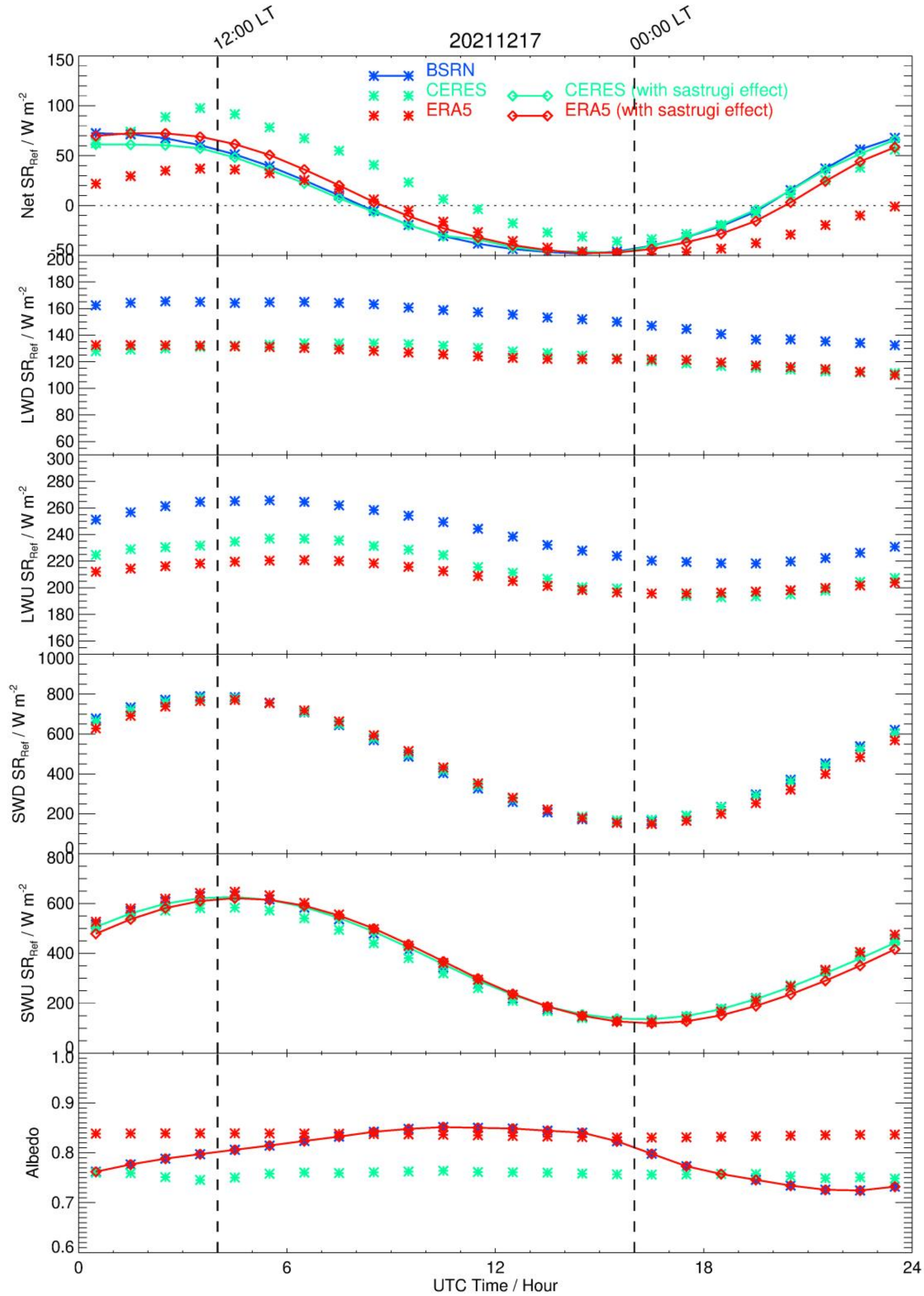

Figure R5. *Same as Figure R1 with the albedo inserted in the lowermost panel. Net SR, SWU SR, and albedo including the sastrugi effect for ERA5 (red solid line) and CERES (green solid line) have also been added in the Figures.*

We have fitted the BSRN albedo averaged over the 5 reference days with the sum of 2 sine functions, imposing periods of 24 and 12 hours. Figure R6 shows the BSRN albedo averaged over the five clear-sky days, the fitted trigonometric function and the residuals between the averaged albedo and the fitted function. We can state that the sastrugi effect on the observed clear-sky albedo at Concordia is successfully fitted by 2 sine functions of 24h and 12h periods to within 0.003 mean absolute error, with a coefficient of determination R^2 equal to 0.993 and a root mean square error of 0.0004.

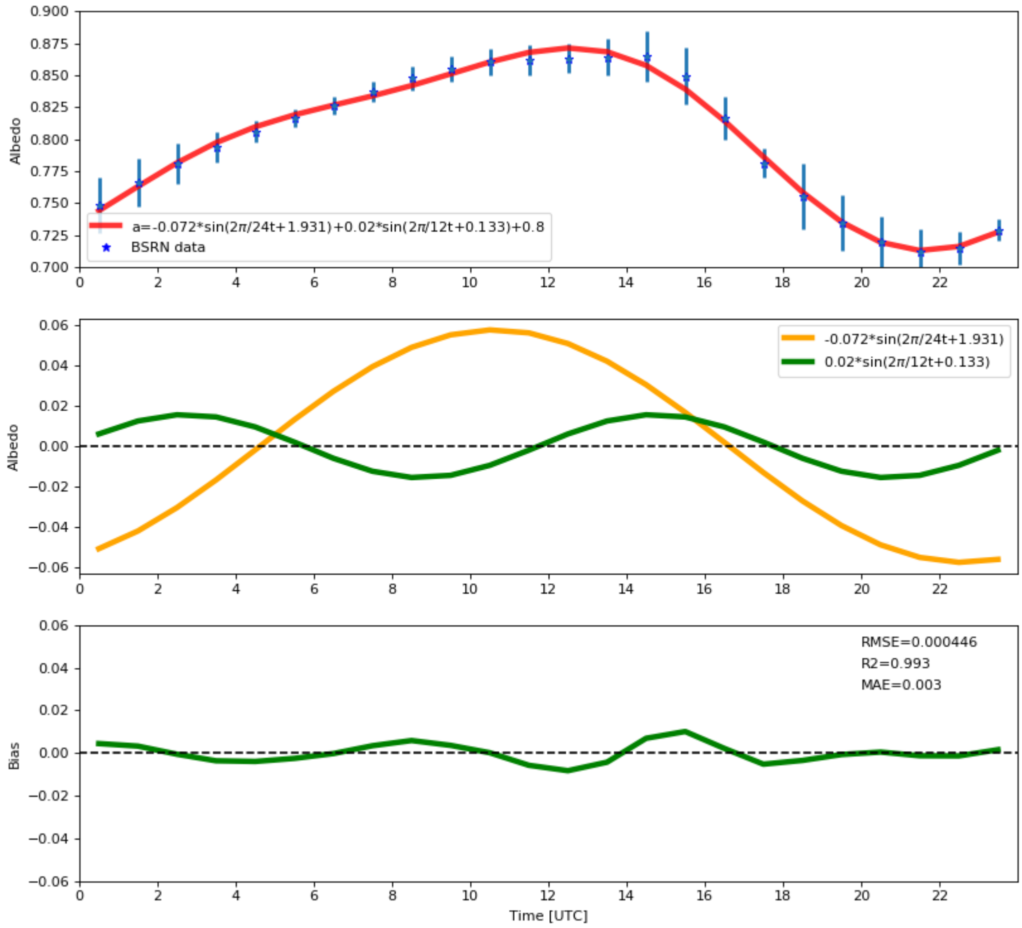

Figure R6. *Top: Hourly time evolution (UTC, hour) of the mean surface albedo (blue stars) with the associated standard deviation (vertical bar) calculated from the BSRN data over the 5 clear-sky days together with the fitted trigonometric function made of two sine functions (red). Center: The two sine functions fitting the BSRN mean surface albedo. Bottom: bias of the fit curve (BSRN-fit) and associated root mean square error (RMSE), coefficient of determination (R^2), and mean absolute error (MAE).*

Moreover, we have considered all the BSRN observations in Decembers 2018, 2019, 2020 and 2021 to calculate the albedo (Figure R7), and we have superimposed the fitted trigonometric function as described in Figure R6. The presence of clouds is well highlighted by observations that depart from the fitted function whilst, during periods of clear-sky conditions, BSRN albedos coincide well with the fitted function.

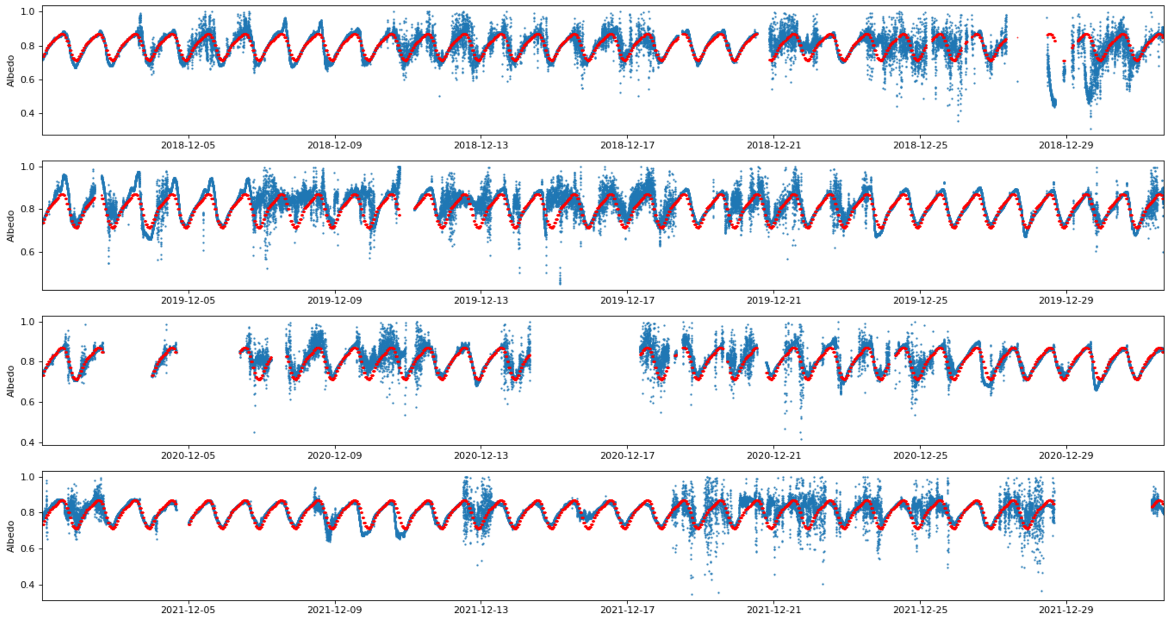

Figure R7. *Hourly time evolution (UTC, hour) of the surface albedo observed by the BSRN instruments (blue), and the two-sine fit (red) for the whole BSRN data set covering the month of December in 2018, 2019, 2020 and 2021.*

5) Conclusions

The study we have performed was extremely fruitful to evaluate the impact of the SLW clouds on the SR. The methodology requires reference clear-sky SR values that can be evaluated from: 1) models, 2) analyses and 3) observations. Our study has mainly shown that, at the Concordia station, sastrugi were present and strongly impacted the net SR via the surface albedo. This very local phenomenon cannot be taken into account by either the global-scale analyses (ERA5 and CERES), or standard radiative transfer models (e.g. RRTMG as suggested by the reviewers). As a consequence, the methodology we have developed based on field observations is likely the most powerful tool to estimate the Net SR in Concordia. It has some drawbacks, as for instance some biases for LWD and LWU between analyses and observations, but the LWD and LWU difference used to calculate the Net SR dramatically lessens the bias.

We have modified the revised version of the manuscript to explain the impact of the sastrugi effect on the SR by adding a detailed new section (see sub-section 5.2) and we have inserted a new paragraph in the abstract and in the conclusion.

Measurement errors: What are the typical measurement errors of the instruments and how do they impact the results of the study? Also, the sometime negative radiation balance should lead to near-surface temperature inversions that are hard to measure with microwave radiometers because the obtained temperature profiles are typically very smooth. How do these inversions impact the results?

→ We kept in the revised manuscript a sub-section “Errors” (5.4) that was already in the submitted manuscript. It is dedicated to measurement errors associated to each instrument. We highlighted the fact that random errors cannot impact on the results presented here because they are divided by $N^{1/2}$ with N the number of observations. It is clear that systematic errors are not altered by the statistics but these errors are extremely difficult to characterize and may provide an explanation of the small biases found. This point has already been discussed.

Regarding temperature, we are not quite sure about the meaning of the question. We select in-cloud temperature to perform our analyses. Since SLW clouds are generally present in an altitude range from 400 to 800 m in December, the near-surface temperature profiles (and more specifically temperature inversion) would have a negligible effect on the observed parameters in the cloud layer.

Minor comments:

General: When discussing temperature, I recommend to be more specific. Is it surface or cloud temperature? Is it potential or regular temperature?

→ This point is presented in detail in the replies to the comments from Reviewer #1 together with the methodology employed. We use in-cloud regular temperature.

L94: Readability would improve if proper notation was used.

→ We have modified the notations accordingly (see in the Introduction).

L236: What is the physical explanation why multiple normal distributions are required?

→ It is rather difficult to give a simple explanation. Considering the SR vs. LWP relationship, it seems that we have systematically one of the Gaussian distributions centred around 0 W m^{-2}, reflecting the non-impacting part of SLWCs on SR components. Considering the temperature vs. LWP relationship, the 2 main Gaussian distributions are centred around -28°C and -30°C, corresponding to temperatures usually encountered in Concordia whilst the third one, far much less intense, is centered around -18°C, probably the signature of very unusual events occurring in Concordia as the warm-moist events associated with atmospheric rivers. We have inserted two paragraphs in the revised manuscript (see sub-section 4.2).

L254: I think the plots show the probability density, but not the probability density function which would be an analytical formula to describe the probability density.

→ Right. We modified the term "Probability Density Function" into "Probability Density".

L261: *joint* Gamma distributions ?

→ We clarified this issue by rewriting the sentence as (see sub-section 4.1):

> We have performed a weighted average of the LWPs within each temperature bin (Figure 6 centre). Then, we have fitted 3 Gaussian distributions to the count numbers as a function of temperature (Figure 6 right). If we now only consider temperature bins within one-sigma of the centre of the Gaussian distributions, we can fit the following logarithmic relation of the temperature θ as a function of LWP within the SLWC (Figure 6 centre):

Similarly, we have modified the sentence related to the Gaussian distribution of SR vs LWP as (see sub-section 4.2):

> The central panel shows, for the same parameters, the corresponding weighted average LWP within 5 W m^{-2}-wide bins of radiation anomaly whereas the right panel shows the corresponding count number within 5 W m^{-2}-wide bins fitted by 2 Gaussian distributions.

L265, L281: add unit to +/- 1.5, +/- 10

→ Done: (±1.5 °C) and (±10.0 W m^{-2})

L267: liquid water *content*

→ Done

L354: What variables would be how impacted by ice contaminated clouds?

→ This point has been dealt in detail while considering a concurring comment from the Reviewer #1. Here is our common response:
→ Microwave observations at 60 and 183 GHz are not sensitive to ice crystals. This has already been discussed in Ricaud et al. (2018) when considering the study of diamond dust in Antarctica. As a consequence, precipitation detected by the Lidar does not affect retrievals of temperature, water vapour and liquid water. Nevertheless, during long episodes of large precipitation that can happen in winter periods, some amount of snow can accumulate on the shield protecting the HAMSTRAD radiometer. In summer time, a technician looks after the instrument and sweeps out the accumulated snow. But in winter, it is much more difficult for a technician to move outside of the base and unfortunately the sweeping may be performed few days after an intensive period of precipitation. As a consequence, snow that accumulates on the HAMSTRAD protective shield can perturb the 183-GHz signal, thus water vapour and LWP retrievals. But we recall that our present analysis is performed for the summer months of December 2018-2021 when precipitation is less intense and manpower very active to look after the instrument. We have added some sentences in the revised manuscript to clarify the issue of precipitation and impact on the LWP retrievals (see sub-section 2.2).

L409ff: Would the mean Net SR be more interesting than the maximum?

→ Since we are interested in the maximum possible impact of SLWC on Net SR, it sounds more logical to study the maximum of Net SR. Moreover, if the impact had appeared to be negligible when considering the maximum Net SR, we could have concluded that the impact of SLWC on the Net SR was limited.

L410: Please provide the mean cloud fraction value.

→ We have inserted a new sentence (see sub-section 5.6):

> In summer, η_{CF} is varying from 5% in Eastern Antarctica to 40% in Western Antarctica whilst, in winter, it is varying from 0% in Eastern Antarctica to 20% in Western Antarctica (Listowski et al., 2019).